Available online at www.sciencedirect.com
SCIENCE DIRECT®
Comput. Methods Appl. Mech. Engrg. 192 (2003) 227–246
Computer methods in applied mechanics and engineering
www.elsevier.com/locate/cma

A level set method for structural topology optimization

Michael Yu Wang [a,*], Xiaoming Wang [b], Dongming Guo [b]

[a] *Department of Automation and Computer-Aided Engineering, The Chinese University of Hong Kong, 405 Mong Wan Wai Building, Shatin, NT, Hong Kong*
[b] *School of Mechanical Engineering, Dalian University of Technology, Dalian 116024, China*

Received 9 July 2002; received in revised form 6 September 2002

Abstract

This paper presents a new approach to structural topology optimization. We represent the structural boundary by a level set model that is embedded in a scalar function of a higher dimension. Such level set models are flexible in handling complex topological changes and are concise in describing the boundary shape of the structure. Furthermore, a well-founded mathematical procedure leads to a numerical algorithm that describes a structural optimization as a sequence of motions of the implicit boundaries converging to an optimum solution and satisfying specified constraints. The result is a 3D topology optimization technique that demonstrates outstanding flexibility of handling topological changes, fidelity of boundary representation and degree of automation. We have implemented the algorithm with the use of several robust and efficient numerical techniques of level set methods. The benefit and the advantages of the proposed method are illustrated with several 2D examples that are widely used in the recent literature of topology optimization, especially in the homogenization based methods.

Keywords: Structural optimization; Shape optimization; Topology optimization; Level set models; Level set method; Implicit moving boundary

1. Introduction

The goal of this paper is to advance methodology for structural topology optimization. We present a powerful method based on *level set models* for optimizing linearly elastic structures which satisfy a design objective and certain constraints. In the proposed method, the structure under optimization is implicitly represented by a moving boundary embedded in a scalar function (the level set function) of a higher dimensionality. While the shape and topology of the structure may undergo major changes, the level set function remains to be simple in its topology. Therefore, by a direct and efficient computation in the embedding space, the movement of the design boundaries under a relevant speed function can be tracked to capture changes in the shape and topology of the structure. The level set models may also be referred to as

* Corresponding author. Tel.: +852-2609-8487; fax: +852-2603-6002.
E-mail address: yuwang@acae.cuhk.edu.hk (M.Y. Wang).

0045-7825/03/$ - see front matter
PII: S0045-7825(02)00559-5

implicit moving boundary (IMB) models and they can easily represent complex boundaries that can form holes, split into multiple pieces, or merge with others to form a single one. Based on the concept of propagation of the level set surface, the design changes are carried out as a mathematical programming for the problem of optimization.

We have developed a numerical procedure for the structural optimization problem using the level set models. Necessary conditions for the optimum solution and for the convergence of the procedure are derived. We have implemented the proposed algorithm with the use of several robust and efficient numerical techniques of level set methods. The benefit and the advantages of the proposed method are illustrated with several 2D examples that are widely used in the recent literature of topology optimization, especially in the homogenization based methods.

2. Background

Structural optimization, in particular the shape and topology optimization, has been identified as one of the most challenging tasks in structural design. Various techniques and approaches have been developed during the past decade. The following is a brief review of the key approaches.

One main approach to structural design for variable topologies is the method of homogenization [1–8], in which a material model with micro-scale voids is introduced and the topology optimization problem is defined by seeking the optimal porosity of such a porous medium using one of the optimality criteria. By transforming the difficult topology design problem into a relatively easier "sizing" problem, the homogenization technique is capable of producing internal holes without prior knowledge of their existence. That is, it offers a tool for simultaneous shape and topology optimization. However, the homogenization method may not yield the intended results for some objectives in the mathematical modeling of structural design. It often produces designs with infinitesimal pores in the materials that make the structure not manufacturable. Further, numerical instabilities may introduce "non-physical" artifacts in the results and make the designs sensitive to variations in the loading.

A number of variations of the homogenization method have been investigated to deal with these issues by penalization of intermediate densities, especially the "solid isotropic material with penalization" approach for its conceptual simplicity [9–11]. Material properties are assumed constant within each element used to discretize the design domain and the design variables are the element densities. The material properties are modeled to be proportional to the relative material density raised to some power. The power-law based approach to topology optimization has been widely applied to problems with multiple constraints, multiple physics and multiple materials. However, numerical instability and computational complexity remain to be the major difficulties for realistic requirements.

A simple method for shape and layout optimization, called "evolutionary structural optimization" (ESO), has been proposed by Xie and co-workers [12,13] which is based on the concept of gradually removing material to achieve an optimal design. The method was developed for various problems of structural optimization including stress considerations, frequency optimization, and stiffness constraints. The ESO method uses a fixed model with standard finite elements to represent the initial design domain while the so-called optimum design is found as a subset of the initial set of finite elements. A key process of this method is to use an appropriate criterion to assess the contribution of each element to the specified behavior (response) of the structure and subsequently to remove some elements with the least contribution (usually known as *hard kill*). This approach is essentially based on an evolutionary strategy focusing on local consequences but not on the global optimum. It is typically computationally expensive. A similar approach called "reverse adaptivity" was proposed by Reynolds et al. [14] at which a fixed percentage of relatively under-stressed material is removed to find approximately fully stressed structures. Essentially, both ESO and reverse adaptivity are homotopy methods based on material hard kills. In reverse adaptivity

finite element meshes near the boundary during the design procedure are refined to reduce computational cost or increase resolution.

Another related approach is called "bubble method" proposed by Eschenauer and co-workers [15,16]. In the method, so-called characteristic functions of the stresses, strains and displacements are employed to determine the placements or insertion of holes of known shape at optimal positions in the structure, thus modifying the structural topology in a prescribed fashion In such case, the design for a given topology is settled before its further changes.

Adopting the same principle of redesigning the structure based on the stress distribution in the current design, another approach was developed by Sethian and Wiegmann [17] with a focus on the resolution of the boundaries. The boundaries are allowed to move according to the stresses on the boundaries. A level set method is employed for tracking the motion of the structural boundaries under a speed function and in the presence of potential topological changes. An explicit jump immersed interface method is used for computing the solution of the elliptic problem in complex geometries without using meshes. The approach is also an evolutionary one. The principal idea is to remove material in regions of low stress and to add material in regions of high stress. A removal rate is established representing a percentage of the maximal initial stress below which material may be eliminated, and above which material should be added. The removal rate determines the closed stress contours along which new holes are cut and also the velocity of the boundary motion. The biggest benefit of this approach is that it is easier to add material (with some subgrid resolution) at holes' boundaries with high stress than on a triangulated finite element mesh. This approach seeks to improve design by making more efficient use of the material. The evolutionary process can be characterized as to allow one to start with a design that has holes cut "in the wrong places" and see these holes disappear.

Boundary-based methods for structural design are another class of methods, also known as shape optimization methods. In a boundary-based optimization problem, the design variables directly control the exterior and interior boundary shapes of the structure. It is a more direct approach than homogenization. For example, in general it allows more explicit representation of any features to be incorporated in the design. However, such a boundary representation often has a sever limitation that it defines a *fixed* topology of the structure. Changes in topology provide the greatest challenge in a boundary-based approach to structural optimization.

In our point of view, a boundary-based method with the capability of handling topology changes has the most promising potential. Our proposed method is to use implicit, moving boundaries for topology optimization. The structural boundaries are viewed as moving during the optimization process—interior boundaries (or holes) may merge with each other or with the exterior boundary and new holes may be created. Our idea is to combine level set methods [17,18] for the representation of the IMBs and a mathematical programming method for topology optimization.

3. Level set models of implicit moving boundaries

In practice, the method of IMBs for structural optimization must be computed using some specific boundary representation. Generally speaking, it is desirable to have the boundary representation as general as the underlying physical theory. More importantly, the representation should not rely on any kind of explicit parameterization, along with no direct specification of the topology of the structure. These capabilities would allow the boundary models to easily change the structural topology while undergoing optimization. A boundary can "split" into pieces to form multiple boundaries. Conversely, several distinct boundaries may come together to make a single boundary. Because of the lack of explicit parameterization, the boundary models do not suffer the problems of parametric surfaces, e.g., a limited set of possible shapes and the need of re-parameterization after undergoing significant changes in shape.

For these reasons we use the method of level set models [18–20] for an implicit representation of the structural boundaries. The fundamental concept of level set methods is described here for a general 3D structure with surface boundaries to provide necessary background for later sections. A level set model specifies a surface in an implicit form as an iso-surface of a scalar function, $\Phi : R^3 \mapsto R$, embedded in 3D, i.e.,

$$S = \{x : \Phi(x) = k\}, \tag{1}$$

where k is the iso-value and is arbitrary, and x is a point in space on the iso-surface Φ. In other words, x is the set of points in R^3 that composes the kth iso-surface of Φ. The embedding Φ can be specified in any specific form, e.g., as a regular sampling on a rectilinear grid. A process of structural optimization can be described by letting the level set function dynamically change in time. Thus, the dynamic model is expressed as

$$S(t) = \{x(t) : \Phi(x(t), t) = k\}. \tag{2}$$

By differentiating both sides of Eq. (2) with respect to time and applying the chain rule, we obtain the so-called "Hamilton–Jacobi-type" equation

$$\frac{\partial \Phi(x,t)}{\partial t} + \nabla \Phi(x,t) \frac{\mathrm{d}x}{\mathrm{d}t} = 0. \tag{3}$$

This equation defines an initial value problem for the time dependent function Φ.

In this dynamic level set model, the structural optimization process can be viewed as follows. Let $\mathrm{d}x/\mathrm{d}t$ be the movement of a point on a surface driven by the objective of the optimization, such that it can be expressed in terms of the position of x and the geometry of the surface at that point. Then, the optimal structural boundary is expressed as a solution of a partial differential equation on Φ:

$$\frac{\partial \Phi(x)}{\partial t} = -\nabla \Phi(x) \frac{\mathrm{d}x}{\mathrm{d}t} \equiv -\nabla \Phi(x) \Gamma(x, \Phi), \tag{4}$$

where $\Gamma(x, \Phi)$ denotes the "speed vector" of the level set surface, which depends on the objective of the optimization.

This formulation with level set models has two major theoretical and practical advantages over conventional surface models, especially in the context of topology optimization. First, level set models are topologically flexible. The 3D scalar function Φ is defined to always have a simple topology; its level sets can easily represent complicated surface shapes that can form holes, split to form multiple boundaries, or merge with other boundaries to form a single surface. There is no need to re-parameterize the model as it undergoes significant changes in shape, in contrast to any conventional boundary shape design [18]. Further, the models can incorporate a large number of degrees of freedom and a number of numerical techniques have been developed [18] to make the initial value problem of Eq. (4) computationally robust and efficient. In fact, the computational complexity can be made proportional to the level set's surface area rather than the size of the volume in which it is embedded. We shall describe the details of our proposed approach and its numerical implementation as follows.

4. The level set formulation

In this section we present a formulation of the level set method for finding the optimum design of a linearly elastic structure. In this context the optimum design of the structure includes information on the topology, shape and sizing of the structure and the level set models allow for addressing all three problems simultaneously.

In the general case, the problem of structural optimization can be specified as

$$\begin{aligned} \underset{\partial D}{\text{Minimize}} \quad & J(u) = \int_D F(u)\,\mathrm{d}\Omega, \\ \text{subject to:} \quad & \int_D E_{ijkl}\varepsilon_{ij}(u)\varepsilon_{kl}(v)\,\mathrm{d}\Omega = \int_D pv\,\mathrm{d}\Omega + \int_{\partial D_t} \tau v\,\mathrm{d}S, \\ & u|_{\partial D_u} = u_0 \quad \forall v \in U, \\ & \int_D \mathrm{d}\Omega \leqslant V_{\max}. \end{aligned} \tag{5}$$

Here, the solid domain of the structure is represented by D with its boundary ∂D. The linearly elastic equilibrium equation is written in its weak variation form, with u denoting the displacement field in the space U of kinematically admissible displacement fields, E_{ijkl} the elasticity tensor, ε_{ij} the strain tensor, p the body forces, τ the boundary tractions applied on the part ∂D_t of the boundary ∂D, and u_0 the prescribed displacement on the part ∂D_u of the ∂D. The last inequality describes an upper limit on the amount of material in terms of the maximum admissible volume $V_{\max}$ of the design domain. The problem of structural optimization is to find the optimal boundary ∂D of D so that the objective function $J(u)$ is minimized for a specific physical or geometric type described by F. This is a standard notion of topology optimization [8].

For an easy embedding of the level set models, we define a larger, fixed reference domain $\overline{D}$ such that it fully contains the current structure solid D, i.e., $D \subseteq \overline{D}$. As described in Eq. (4), the structural boundary ∂D is to be represented implicitly by a level set model S as an embedding through a higher dimensional function $\Phi(x)$ such that $S = \{x : x \in \overline{D},\ \Phi(x) = 0\}$. Here we use the convention that $k = 0$. Furthermore, we define an inside–outside function for Φ such that

$$\Phi(x) > 0 \quad \forall x \in D \setminus \partial D, \tag{6}$$

$$\Phi(x) < 0 \quad \forall x \in \overline{D} \setminus D. \tag{7}$$

These domains and the level set embedding of the model are shown in Fig. 1.

Thus, with the level set models we can formulate the optimal design problem as follows:

$$\begin{aligned} \underset{\Phi}{\text{Minimize}} \quad & J(u,\Phi) = \int_{\overline{D}} F(u)H(\Phi)\,\mathrm{d}\Omega, \\ \text{subject to:} \quad & a(u,v,\Phi) = L(v,\Phi), u|_{\partial D_u} = u_0, \quad \forall v \in U, \\ & V(\Phi) \leqslant V_{\max} \end{aligned} \tag{8}$$

in terms of the energy bilinear form $a(u,v,\Phi)$, the load linear form $L(v,\Phi)$, and the volume $V(\Phi)$ of the structure, respectively described by

$$\begin{aligned} a(u,v,\Phi) &= \int_{\overline{D}} E_{ijkl}\varepsilon_{ij}(u)\varepsilon_{kl}(v)H(\Phi)\,\mathrm{d}\Omega, \\ L(v,\Phi) &= \int_{\overline{D}} pvH(\Phi)\,\mathrm{d}\Omega + \int_{\overline{D}} \tau v\delta(\Phi)|\nabla\Phi|\,\mathrm{d}\Omega, \\ V(\Phi) &= \int_{\overline{D}} H(\Phi)\,\mathrm{d}\Omega, \end{aligned} \tag{9}$$

where $\delta(x)$ is the Dirac function and $H(x)$ is the Heaviside function.

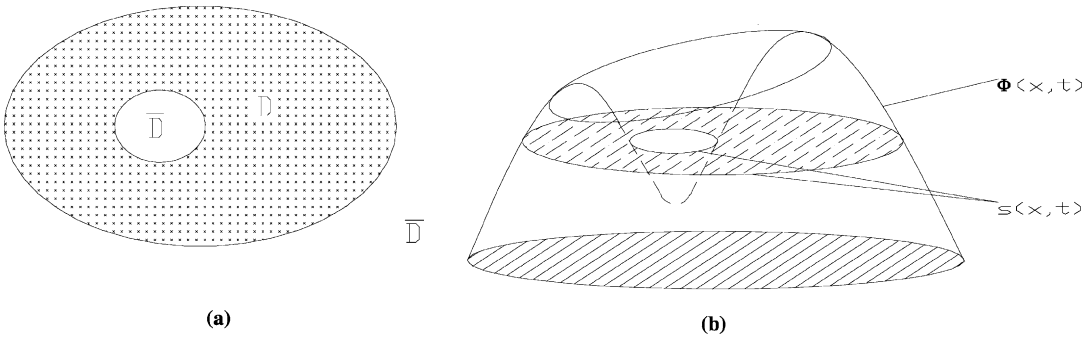

Fig. 1. Design domains and the level set model: (a) designed solid D and its embedding domain $\overline{D}$ and (b) embedded function $\Phi(x)$ and level set model S.

5. Optimization algorithm

With the formulation of Eq. (8) we now describe an optimization procedure. The optimization process operates on the scalar function Φ which is defined over the fixed domain $\overline{D}$. The process can be implemented as a mathematical programming problem. The principal guideline for the optimization process is to move the design boundary represented by the level set model according to its variation sensitivities with respect of the objective function. The process would terminate when the objective cannot be improved further. This optimization procedure is derived from the fundamentals of curve and surface evolution of the level set methods [18] in terms of evolution of the level set surfaces described by Eq. (4). The key development of our application of the level set methods here is to find an appropriate "speed vector" (Γ in Eq. (4)) such that it will drive the design boundary into the optimum shape based on the given objective function and the constraints. As shown in Eq. (4) the speed vector must be expressed in terms of the shape of the boundary and the variation sensitivity. At the optimum solution the boundary variation sensitivity everywhere on the boundary is identical. A highlight of our approach presented here is the identification of the speed vector as the link between the general structural optimization process and the powerful methods of level sets. Our optimization algorithm is described as follows.

Optimization Algorithm:

Step 1: Initialize the embedding level set function $\Phi(x,0)$ at $t=0$. A general treatment is to set $\Phi(x)$ to be the signed distance to the given boundary of the initial design D such that $\Phi(x)=0\ \forall x\in\partial D$. The equilibrium equation is then solved to find the displacement u:

$$a(u,v,\Phi)=L(v,\Phi),\qquad u|_{\partial D_u}=u_0(x),\quad \forall v\in U. \tag{10}$$

Step 2: Find the adjoint displacement w of the conjugate equation:

$$a(v,w,\Phi)=\langle J_u(u,\Phi),v\rangle,\qquad w|_{\partial D_u}=0,\quad \forall v\in U. \tag{11}$$

Here $\langle J_u(u,\Phi),v\rangle$ denotes the Fréchet derivative of $J(u,\Phi)$ with respect to u in the direction of $v(x)$ and it is written as

$$\langle J_u(u,\Phi),v\rangle=\int_{\overline{D}}\frac{\partial F(u)}{\partial u}vH(\Phi)\,\mathrm{d}\Omega.$$

Step 3: Choose a weighting function $\mu(x)\neq 0$ in the fixed reference domain $\overline{D}$ and calculate the Lagrange multiplier λ_+ of the volume constraint of the structure:

$$\begin{aligned}
&\lambda = -\frac{\int_{\overline{D}} \mu^{-2}(x)\beta(u,w,\Phi)\delta(\Phi)|\nabla\Phi|\,\mathrm{d}\Omega}{\int_{\overline{D}} \mu^{-2}(x)\delta(\Phi)|\nabla\Phi|\,\mathrm{d}\Omega},\\
&\lambda_+ = \max[\lambda, 0], \quad \mu(x) \neq 0 \ \ \forall x \in \overline{D},\\
&\beta(u,w,\Phi) = F(u) + pw - \tau w \nabla\left(\frac{\nabla\Phi}{|\nabla\Phi|}\right) - E_{ijkl}\varepsilon_{ij}(u)\varepsilon_{kl}(w),
\end{aligned} \tag{12}$$

where $\beta(u,w,\Phi)$ describes the sensitivity of the objective function $J(u,\Phi)$ with respect to the boundary variation of the design.

Step 4: Calculate "speed function" $V_n(x)$ which defines the "speed" of propagation of all level sets of the embedding function $\Phi(x)$ along the normal direction N of the IMB. In other words, we let $V_n(x) \equiv (\mathrm{d}x/\mathrm{d}t)N(x) = -\Gamma(x,\Phi)N(x)$ (see Eq. (4)). This speed function is defined to satisfy the following equation:

$$-\int_{\overline{D}} (\beta(u,w,\Phi) + \lambda_+)\delta(\Phi)\Psi(x)\,\mathrm{d}\Omega = \int_{\overline{D}} \mu^2(x)V_n(x)\Psi(x)\,\mathrm{d}\Omega \tag{13}$$

for any continuous function $\Psi(x) \in C^0(\overline{D})$.

Step 5: Solve the following standard level set equation to update the embedding function $\Phi(x,t)$:

$$\begin{aligned}
&\frac{\partial\Phi}{\partial t} = V_n(x)|\nabla\Phi|,\\
&\frac{\partial\Phi}{\partial n}|_{\partial\overline{D}} = 0.
\end{aligned} \tag{14}$$

Step 6: Check if a termination condition is satisfied. If the condition is met, then a convergent solution is found. Otherwise, repeat Steps 1–5 until convergence. The termination condition is defined as

$$\int_{\overline{D}} |V_n(x)|\delta(\Phi)|\nabla\Phi|\,\mathrm{d}\Omega \leqslant \gamma,$$

where γ is a specified error limit.

6. Conditions of the optimum solution

In this section we shall derive the necessary conditions for the optimum solution of Eq. (5) and show the convergence characteristics of the algorithm described above. The topology optimization algorithm is developed based on the following proposition:

Proposition 1. *The series of embedding function* $\{\Phi(x,t_i),\ i = 0,1,2,\ldots\}$ *generated by the process of the optimization algorithm are the descent series of the topology optimization problem* (5).

We shall describe a proof of the proposition. First, we derive the Fréchet derivatives of the functions in the optimization problem (8). For the energy bilinear form $a(u,v,\Phi)$, the linear load form $L(v,\Phi)$, and the volume measure $V(\Phi)$, their Fréchet derivatives are respectively given as

$$\left\langle \frac{\partial a(u,v,\Phi)}{\partial\Phi}, \Psi \right\rangle = \int_{\overline{D}} \delta(\Phi)E_{ijkl}\varepsilon_{ij}(u)\varepsilon_{kl}(v)\Psi\,\mathrm{d}\Omega, \tag{15}$$

$$\left\langle \frac{\partial a(u,v,\Phi)}{\partial u}, \delta u \right\rangle = a(\delta u, v, \Phi), \tag{16}$$

$$\left\langle \frac{\partial L(v,\Phi)}{\partial \Phi}, \Psi \right\rangle = \int_{\overline{D}} \delta(\Phi) pv \Psi \, \mathrm{d}\Omega + \int_{\overline{D}} \left(\delta'(\Phi) |\nabla \Phi| \Psi + \delta(\Phi) \frac{\nabla \Phi \nabla \Psi}{|\nabla \Phi|} \right) \mathrm{d}\Omega$$
$$= \int_{\overline{D}} \delta(\Phi) \left(pv - \tau v \nabla \left(\frac{\nabla \Phi}{|\nabla \Phi|} \right) \right) \Psi \, \mathrm{d}\Omega + \int_{\overline{D}} \frac{\delta(\Phi)}{|\nabla \Phi|} \frac{\partial \Phi}{\partial n} \Psi \, \mathrm{d}\Omega, \tag{17}$$

$$\left\langle \frac{\partial V(\Phi)}{\partial \Phi}, \Psi \right\rangle = \int_{\overline{D}} \delta(\Phi) \Psi \, \mathrm{d}\Omega. \tag{18}$$

For the objective function $J(u,\Phi)$ its Fréchet derivatives are specified as:

$$\left\langle \frac{\partial J(u,\Phi)}{\partial \Phi}, \Psi \right\rangle = \int_{\overline{D}} \delta(\Phi) F(u) \Psi \, \mathrm{d}\Omega, \tag{19}$$

$$\left\langle \frac{\partial J(u,\Phi)}{\partial u}, \delta u \right\rangle = \int_{\overline{D}} \frac{\partial F(u)}{\partial u} H(\Phi) \, \delta u \, \mathrm{d}\Omega \tag{20}$$

for any continuous function $\Psi(x) \in C^0(\overline{D})$.

In order to express Eq. (20) as a function of Ψ explicitly, we solve the following conjugate equation and obtain the adjoint displacement field w:

$$a(v,w,\Phi) = \int_{\overline{D}} \frac{\partial F(u)}{\partial u} H(\Phi) v \, \mathrm{d}\Omega, \quad w|_{\partial D_u} = 0 \ \ \forall v \in U. \tag{21}$$

Thus, differentiating the equilibrium equation $a(u,v,\Phi) = L(v,\Phi)$ with respect to Φ in the direction of Ψ, we obtain:

$$a(\delta u, v, \Phi) = \left\langle \frac{\partial L(v,\Phi)}{\partial \Phi}, \Psi \right\rangle - \left\langle \frac{\partial a(u,v,\Phi)}{\partial \Phi}, \Psi \right\rangle. \tag{22}$$

Substituting Eqs. (15), (17), (21) and (22) into (20) yields:

$$\left\langle \frac{\partial J(u,\Phi)}{\partial u}, \delta u \right\rangle = \int_{\overline{D}} \delta(\Phi) \left(pv - \tau v \nabla \left(\frac{\nabla \Phi}{|\nabla \Phi|} \right) - E_{ijkl} \varepsilon_{ij}(u) \varepsilon_{kl}(w) \right) \Psi \, \mathrm{d}\Omega + \int_{\overline{D}} \frac{\delta(\Phi)}{|\nabla \Phi|} \frac{\partial \Phi}{\partial n} \Psi \, \mathrm{d}\Omega. \tag{23}$$

Using the Lagrange multiplier method, we construct another objective function $\overline{J}(u,\Phi)$ and obtain a completely equivalent problem to the original optimization problem (8) as follows:

$$\begin{aligned} &\underset{\Phi}{\text{Minimize}} \quad && \overline{J}(u,\Phi) = J(u,\Phi) + \lambda_+ (V(\Phi) - V_{\max}), \\ &\text{subject to:} && a(u,v,\Phi) = L(v,\Phi), \quad u|_{\partial D_u} = u_0, \ \ \forall v \in U, \\ & && \lambda_+ (V(\Phi) - V_{\max}) = 0, \\ & && \lambda_+ \geqslant 0. \end{aligned} \tag{24}$$

Here λ_+ is the Lagrange multiplier and last two constraints define a complementarity condition: When the inequality of $V(\Phi) < V_{\max}$ is true, then $\lambda_+ = 0$; Otherwise when $V(\Phi) = V_{\max}$, $\lambda_+ > 0$. Thus, the Fréchet derivative of the new objective function $\overline{J}(u,\Phi)$ becomes

$$\left\langle \frac{\mathrm{d}\overline{J}(u,\Phi)}{\mathrm{d}\Phi}, \Psi \right\rangle = \left\langle \frac{\partial J(u,\Phi)}{\partial u}, \delta u \right\rangle + \left\langle \frac{\partial J(u,\Phi)}{\partial \Phi}, \Psi \right\rangle + \lambda_+ \left\langle \frac{\partial V(\Phi)}{\partial \Phi}, \Psi \right\rangle. \tag{25}$$

Substituting the relations (18), (19) and (23) into (25) leads to

$$\left\langle \frac{\mathrm{d}\overline{J}(u,\Phi)}{\mathrm{d}\Phi}, \Psi \right\rangle = \int_{\overline{D}} \delta(\Phi)\left(F(u) + pw - \tau w \nabla\left(\frac{\nabla\Phi}{|\nabla\Phi|} \right) - E_{ijkl}\varepsilon_{ij}(u)\varepsilon_{kl}(w) + \lambda_+ \right)\Psi \,\mathrm{d}\Omega + \int_{\partial\overline{D}} \frac{\delta(\Phi)}{|\nabla\Phi|}\frac{\partial\Phi}{\partial n}\Psi \,\mathrm{d}\Gamma = \int_{\overline{D}} \delta(\Phi)(\beta(u,w,\Phi) + \lambda_+)\Psi \,\mathrm{d}\Omega + \int_{\partial\overline{D}} \frac{\delta(\Phi)}{|\nabla\Phi|}\frac{\partial\Phi}{\partial n}\Psi \,\mathrm{d}\Gamma. \tag{26}$$

Thus, the Kuhn–Tucker condition of the optimization becomes

$$\begin{aligned} &\beta(u,w,\Phi) + \lambda_+|_{\partial D} = 0, \quad \left.\frac{\partial\Phi}{\partial n}\right|_{\partial\overline{D}} = 0, \\ &\lambda_+(V(\Phi) - V_{\max}) = 0, \quad \lambda_+ \geqslant 0. \end{aligned} \tag{27}$$

Let us choose a weighting function $\mu(x) \neq 0 \,\forall x \in \overline{D}$. We then can construct the speed function $V_n(x)$ as follows:

$$\int_{\overline{D}} \mu^2(x) V_n(x)\Psi \,\mathrm{d}\Omega = -\int_{\overline{D}} \delta(\Phi)(\beta(u,w,\Phi) + \lambda_+)\Psi \,\mathrm{d}\Omega \quad \text{and} \quad V_n|_{\partial\overline{D}} = 0, \quad \forall \Psi \in C^0(\overline{D}). \tag{28}$$

This speed function $V_n(x)$ represents a non-local version of the exact sensitivity function (26) of the optimization problem (24). Therefore, the series $\{\Phi(x,t_i)\}$ generated by using the following Hamilton–Jacobi equation are the descent series of the optimization problem (5),

$$\frac{\partial\Phi}{\partial t} = V_n|\nabla\Phi|, \qquad \left.\frac{\partial\Phi}{\partial n}\right|_{\partial\overline{D}} = 0. \tag{29}$$

As shown in Fig. 2, these equations define the movement of the level set models only along the normal direction of the structural boundary driven by the normal speed V_n.

To finish off the proof we can determine the Lagrange multiplier λ_+ using the Kuhn–Tucker condition (27). When $\lambda_+ \neq 0$, the constant volume condition $\mathrm{d}V(\Phi)/\mathrm{d}t = 0$ leads to

$$\int \delta(\Phi) V_n |\nabla\Phi| \,\mathrm{d}\Omega = 0. \tag{30}$$

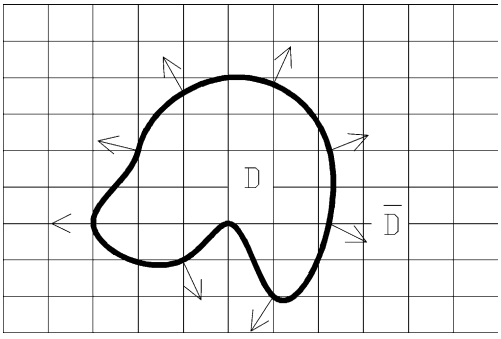

Fig. 2. The movement of the structural boundary.

Substituting Eq. (28) into Eq. (30) yields

$$\int_{\overline{D}} \delta^2(x)\mu^{-2}(x)(\beta(u,w,\Phi)+\lambda_+)|\nabla\Phi|\,\mathrm{d}\Omega = 0. \tag{31}$$

Thus, we can obtain the Lagrange multiplier

$$\lambda_+ = -\frac{\int_{\overline{D}} \delta(\Phi)\mu^{-2}(x)\beta(u,w,\Phi)|\nabla\Phi|\,\mathrm{d}\Omega}{\int_{\overline{D}} \delta(\Phi)\mu^{-2}(x)|\nabla\Phi|\,\mathrm{d}\Omega}. \tag{32}$$

If Eq. (32) gives the multiplier that $\lambda_+ < 0$, we must set $\lambda_+ = 0$ according to the single sided constraint condition (24) or the Kuhn–Tucker condition (27).

Now, we derive the time derivative of the objective function of optimization (5) using Eqs. (19), (23) and (29):

$$\frac{\mathrm{d}J(u,\Phi)}{\mathrm{d}t} = \left\langle \frac{\partial J(u,\Phi)}{\partial u}, \frac{\partial \Phi}{\partial t} \right\rangle + \left\langle \frac{\partial J(u,\Phi)}{\partial \Phi}, \frac{\partial \Phi}{\partial t} \right\rangle = \int \delta(\Phi)\beta(u,w,\Phi)V_n|\nabla\Phi|\,\mathrm{d}\Omega. \tag{33}$$

When applying Eq. (28), Eq. (33) becomes

$$\frac{\mathrm{d}J(u,\Phi)}{\mathrm{d}t} = -\int_{\overline{D}} \mu^2(x)V_n^2(x)|\nabla\Phi|\,\mathrm{d}\Omega - \lambda_+ \int_{\overline{D}} \delta(\Phi)V_n(x)|\nabla\Phi|\,\mathrm{d}\Omega. \tag{34}$$

Considering the Kuhn–Tucker condition (27) and the volume constraint (30), the last term in Eq. (34) is given to equal to zero. Thus, we conclude that

$$\frac{\mathrm{d}J(u,\Phi)}{\mathrm{d}t} \leqslant 0. \tag{35}$$

Here, the equality holds only for $\delta(\Phi)V_n = 0$. This concludes our proof for Proposition 1.

Furthermore, if we choose $\mu(x)$ to be the kernel function of Φ and the kernel function is assumed to be a soft type of the Dirac function such as the Gauss function, then the kernel characteristic parameter will approach to zero in the series. This means that we can obtain the optimum conditions of the optimization problem (5) from Eqs. (27) and (34) as follows:

$$\beta(u,w,\Phi) + \lambda_+|_{\partial D} = 0. \tag{36}$$

Thus,

$$\lambda_+ = -\int_{\partial D} \beta(u,w,\Phi)\,\mathrm{d}S \Big/ \int_{\partial\overline{D}} \mathrm{d}S$$

and λ_+ becomes the average of the sensitivity $\beta(u,w,\Phi)$ along the entire design boundary ∂D. Moreover, we may rewrite the boundary variation sensitivity $\beta(u,w,\Phi)$ as

$$\beta(u,w,\Phi) = F(u) + pw - \tau w\kappa - E_{ijkl}\varepsilon_{ij}(u)\varepsilon_{kl}(w), \tag{37}$$

where $\kappa = \nabla(\nabla\Phi/|\nabla\Phi|)$ and it is the mean curvature of the boundary surface. Therefore, we have the following proposition.

Proposition 2. *The necessary condition of the optimum solution to the topology optimization problem* (5) *is that the boundary sensitivity* $\beta(u,w,\Phi)$ *keeps a constant everywhere on the boundary of the optimum structure* D.

7. Numerical implementation

There are a number of numerical issues that are important to the implementation of the proposed level set method. In the algorithm presented here, the geometric boundary of the structure under optimization is

described as the zero level set of $\Phi(x,t)=0$. In its numerical implementation, the embedding function Φ may be represented in any convenient form. It is often described as a rectangular sampling on a rectilinear grid of x over $\overline{D}$ [18]. Conventional interpolation functions may be used on a set of grid nodes, such as

$$\Phi(x,t)=\sum_i \phi_i(t)N_i(x), \tag{38}$$

where $\phi_i(t)$ are the nodal values of the level set function and $N_i(x)$ describe the standard interpolation functions. The nodal values are updated during the optimization procedure.

In general, the linear elastic equation (10) may be solved by a finite element method. In order to avoid regenerating the element mesh when the boundary or $\Phi(x,t)$ is modified or updated in the iterative process, we use approximate functions for $\delta(x)$ and $H(x)$ as follows:

$$\delta(x)=\begin{cases}\dfrac{3(1-\alpha)}{4\Delta}\left(1-\dfrac{x^2}{\Delta^2}\right), & |x|\leqslant\Delta,\\ 0, & |x|>\Delta,\end{cases} \tag{39}$$

$$H(x)=\begin{cases}\alpha, & x<-\Delta,\\ \dfrac{3(1-\alpha)}{4}\left(\dfrac{x}{\Delta}-\dfrac{x^3}{3\Delta^3}\right)+\dfrac{1+\alpha}{2}, & -\Delta\leqslant x<\Delta,\\ 1, & x\geqslant\Delta,\end{cases} \tag{40}$$

where α is a small positive number to ensure that the numerical stiffness of Eq. (10) is nonsingular, and Δ describes the width of numerical approximation for $\delta(x)$ and $H(x)$ as shown in Fig. 3.

Another issue is the discrete solution of the Hamilton–Jacobi equation (14). A highly robust and accurate computational method was developed by Osher and Sethian [19] to address the problem of overshooting. Based on the notion of weak solutions and entropy limits, a so called "up-wind scheme" is proposed to solve Eq. (14) with the following update equation

$$\phi_{ijk}^{n+1}=\phi_{ijk}^{n}-\Delta t[\max(V_{n_{ij}},0)\nabla^{+}+\min(V_{n_{ij}},0)\nabla^{-}] \tag{41}$$

with

$$\nabla^{+}=[\max(D_{ijk}^{-x},0)^2+\min(D_{ijk}^{+x},0)^2+\max(D_{ijk}^{-y},0)^2+\min(D_{ijk}^{+y},0)^2+\max(D_{ijk}^{-z},0)^2+\min(D_{ijk}^{+z},0)^2],$$

$$\nabla^{-}=[\max(D_{ijk}^{+x},0)^2+\min(D_{ijk}^{-x},0)^2+\max(D_{ijk}^{+y},0)^2+\min(D_{ijk}^{-y},0)^2+\max(D_{ijk}^{+z},0)^2+\min(D_{ijk}^{-z},0)^2].$$

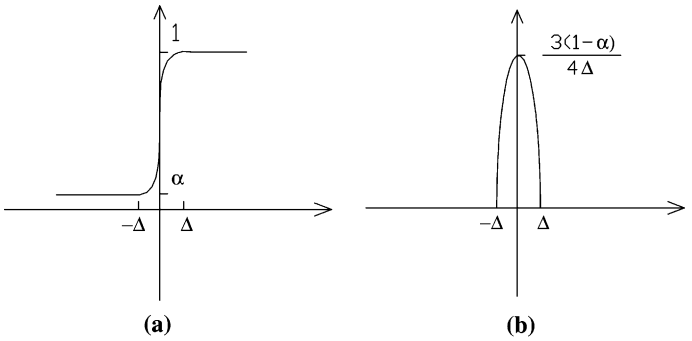

Fig. 3. Numerically approximated (a) Heaviside function $H(x)$ and (b) Dirac function $\delta(x)$.

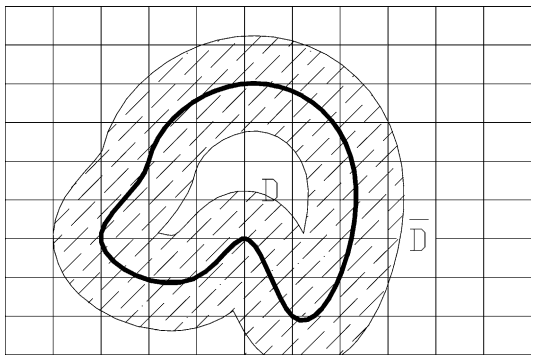

Fig. 4. The narrow band of a level set of interest in a 2D case.

Here, Δt is the time step, and $D_{ijk}^{\pm x}$, $D_{ijk}^{\pm y}$ and $D_{ijk}^{\pm z}$ are the respective forward and back difference operators in the three dimensions of $x \in R^3$ separately. In addition, the time steps Δt must be limited to ensure the stability of the up-wind scheme (41). The Courant–Friedrichs–Lewy condition requires Δt to satisfy

$$\Delta t \max |V_{n_{ijk}}| \leqslant \Delta s, \tag{42}$$

where Δs stands for the minimum grid space among the three dimensions [18]. Furthermore, in order to obtain highly accurate numerical results, the level set function $\Phi(x,t)$ is often initialized as the signed distance function and satisfies the Eikonal equation

$$|\nabla \Phi(x,t)| = 1. \tag{43}$$

The up-wind solutions produce the motion of level set models over the entire range of the embedding, i.e., for all values of Φ in (14). Since the optimum structural boundary is defined to be a single model, i.e., at $k = 0$, the calculation of solutions over the entire range of iso-values is unnecessary. This forms the basis for "narrow-band" schemes that solve Eq. (14) in a narrow band of the grid nodes that surround the level set of interest [18–21], as illustrated in Fig. 4. While the up-wind scheme makes the level set method numerically robust, the narrow-band scheme makes its computational complexity proportional to the boundary area of the structure being optimized rather than the size of the volume in which it is embedded. These two major numerical techniques make the level set method practically attracting. A complete discussion of these schemes may be found in the literature of level set methods (e.g., [18–21]).

8. Numerical examples

In this section we present several examples of structural optimization obtained with the proposed algorithm and implementation. The optimization problem of choice is the mean compliance problem that has been widely studied in the relevant literature (e.g., [8,22]). The objective function of the problem is the strain energy of the structure with a material volume constraint, i.e.,

$$J(u) = \int_D E_{ijkl}\varepsilon_{ij}(u)\varepsilon_{kl}(u)\,\mathrm{d}\Omega. \tag{44}$$

For all examples, the material used is steel with a modulus of elasticity of 210 GPa and a Poisson's ratio of $v = 0.3$. For clarity in presentation, the examples are in 2D ($x \in R^2$) under plane stress condition. For all

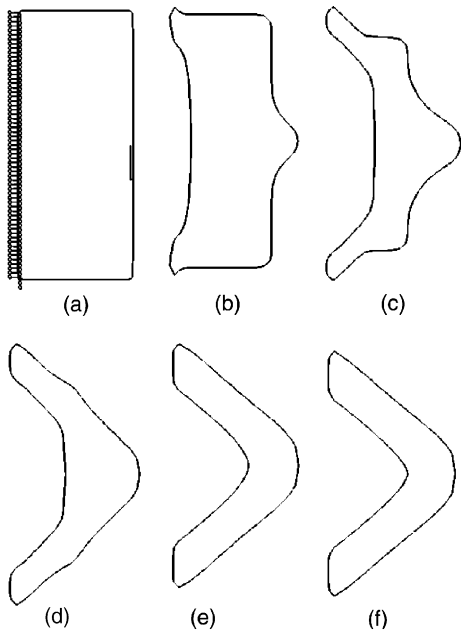

Fig. 5. Results of the iteration in the level set optimization for the two-bar example with a solid initial design without any holes.

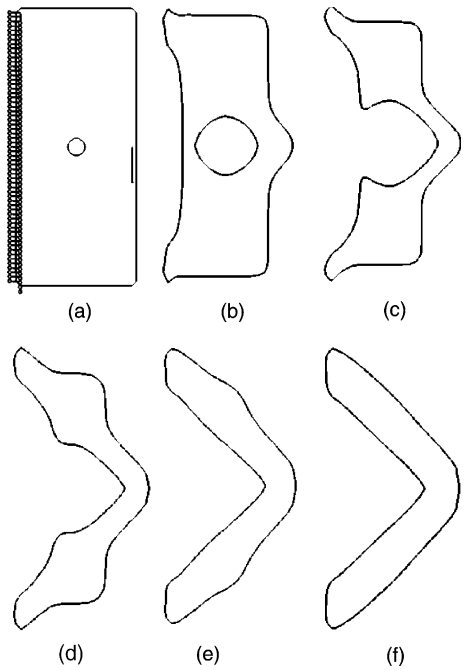

Fig. 6. Results of the iteration in the level set optimization for the two-bar example with a single hole in the initial design.

cases, we use $\alpha = 10^{-9}$ and $\Delta = 2$ in the numerical approximation of $H(x)$ and $\delta(x)$ (Fig. 3). In the implicit description for the level set function Φ, the finite element nodes are used as the nodes of Φ and interpolation functions similar to those of the finite element analysis are also used for Φ. In the narrow-band scheme, the width of the computation band for Φ is set at two-grid length (Fig. 4).

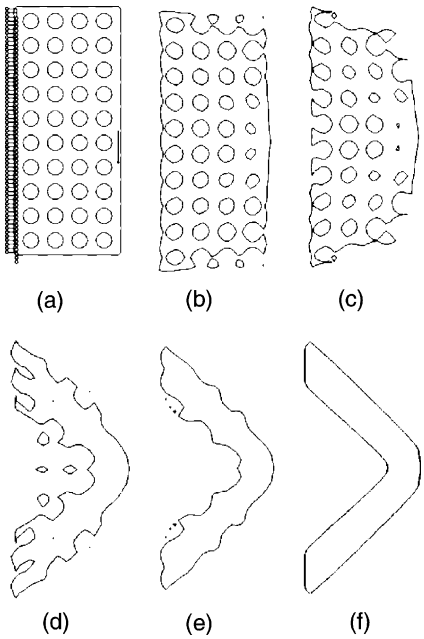

Fig. 7. Results of the iteration in the level set optimization for the two-bar example with a perforated initial design.

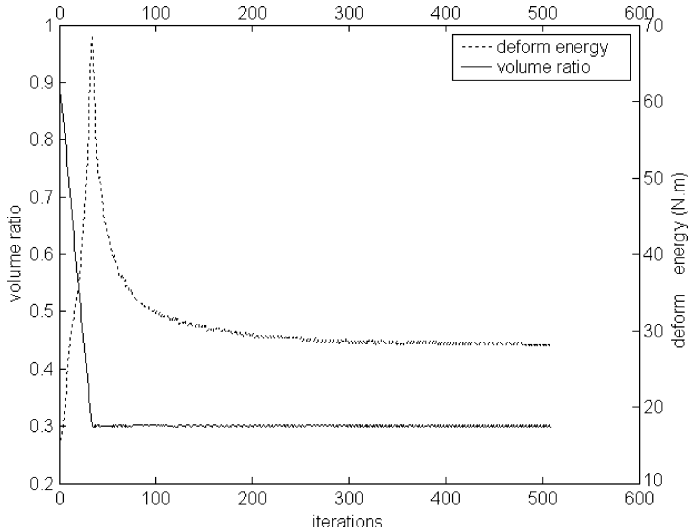

Fig. 8. The strain energy and the volume ratio of the sequence of iterations for case of Fig. 5.

8.1. Two-bar frame

As a verification of the structural optimization algorithm developed here, a simple classic problem of two-bar frame is considered first. For this problem, its optimum-topology solution is known analytically to consist of two beams at 45° to support the applied load to the fixed boundary wall. As shown in Fig. 5(a), the design domain for the structural layout is a rectangular area of 2000 mm in height and 1000 mm in width. A load of 40 kN is applied at the middle of the right edge. The volume ratio of the final design is constrained to be 30%. For this example, a mesh of 62×27 elements is used.

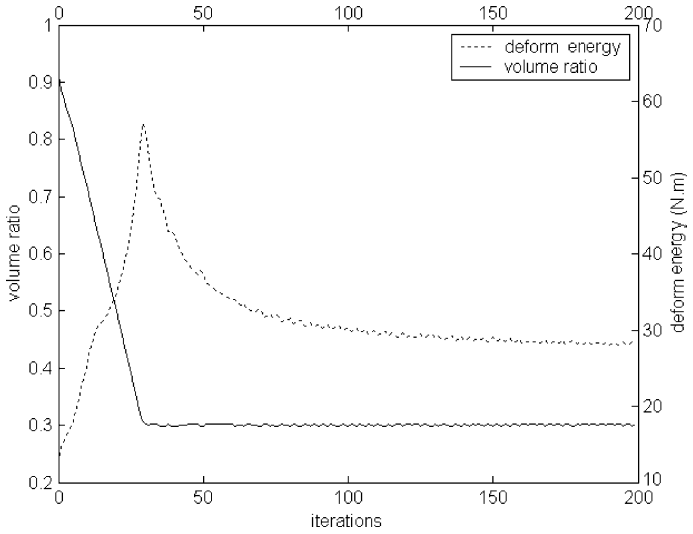

Fig. 9. The strain energy and the volume ratio of the sequence of iterations for case of Fig. 6.

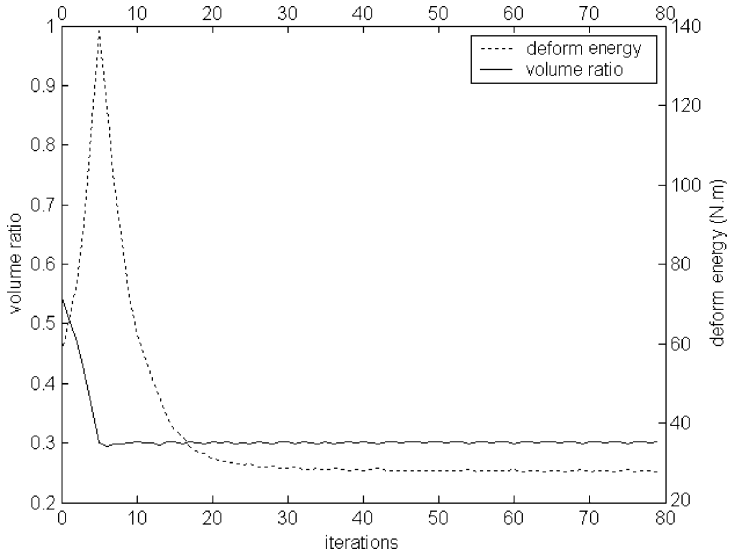

Fig. 10. The strain energy and the volume ratio of the sequence of iterations for case of Fig. 7.

Three different initial conditions are used for the level set based optimization. In the first case, the initial embedding, $\Phi(x,0)$, is set to be the complete domain of design of Fig. 5(a). The optimization process automatically generates a hole as shown in Fig. 5(b), and the exterior and interior boundary shapes are simultaneously changed. Fig. 5(b)–(e) shows some intermediate results of optimization iterations. The final solution shown in Fig. 5(f) is identical to the analytical solution.

Next, a small hole is introduced in the initial design as shown in Fig. 6(a). During the process of optimization, an internal hole is again automatically generated while the existing interior and exterior boundaries of the structure would evolve according to the level set speed function (Fig. 6(b)). The two holes would then meet each other and merge into a single hole as shown in Fig. 6(c). This clearly illustrates the power of the level set model to handle topological changes as well as shape changes during the course of optimization. The process continues until the same final result is achieved (Fig. 6(f)).

It is experienced that the level set model converges to an optimum solution faster with an initial condition of interior holes. In the third case of this example, 40 holes are uniformly distributed in the initial

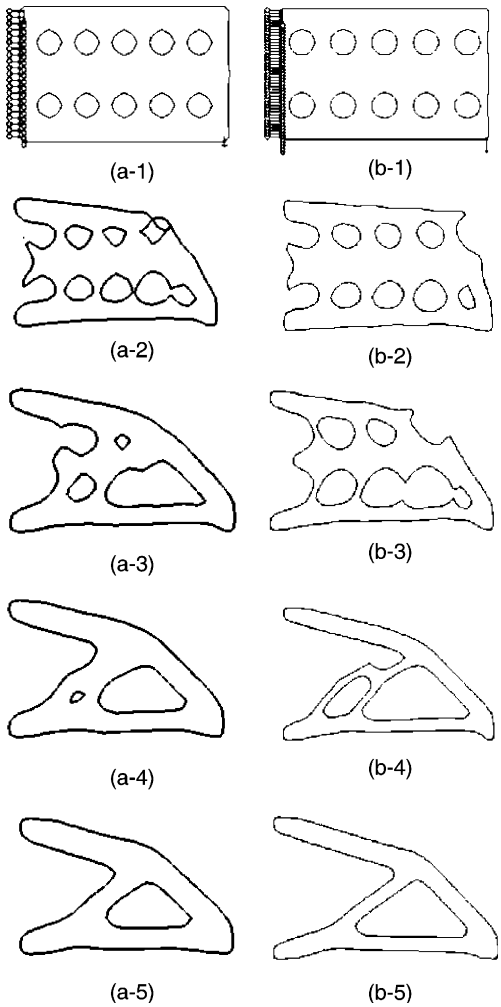

Fig. 11. The optimization results for a cantilever beam: (a) volume ratio of 0.4 and (b) volume ratio of 0.3.

design as shown in Fig. 7(a), representing an original perforated structure. During the process of optimization, many of these holes would merge yielding "Swiss-cheese" structures during iteration (Fig. 7(b)–(e)). In the intermediate steps, some pieces of the structure may also break off to become separated. However, they are eventually evolved to disappear (Fig. 7(d) and (e)), since they are physically meaningless. Again, this illustrates the flexibility and the power of the level set model to handle drastic topological changes. The process continues until the same final result is achieved (Fig. 7(f)).

For these three cases of different initial designs, we further illustrate the changes of the objective function and the structure volume over the iteration, in Figs. 8–10 respectively. In all three cases, it is noted that the optimization process reduces the structural volume in the early iterations to the specified lower limit. Then, while the volume constraint is enforced, the mean compliance is minimized. It is interesting to point out that the level set model converges faster with more perforations in the initial design. It takes about 80 iterations (Fig. 10) for the Swiss-cheese initial design of Fig. 7, compared to about 500 iterations (Fig. 8) for the solid initial design of Fig. 5. In other words, the Swiss-cheese holes are "easier" to be "gobbled up" by the level set evolution than a solid piece when the volume of the structure has to be reduced.

8.2. Cantilever beam

A cantilever beam of ratio 3:2 is loaded vertically at the bottom of its free end as shown in Fig. 11. Two volume ratio constraints of 0.4 and 0.3 are considered respectively. Their initial designs and optimization results are shown in Fig. 11(a:1–5) for 0.4 volume ratio and in Fig. 11(b:1–5) for 0.3 volume ratio respectively. The final optimum solutions are nearly identical to what other researchers have obtained using a homogenization based method (see [8,22]). A mesh of 32×22 elements is used.

8.3. MBB beam

The third example is an MBB beam which is also a benchmark example in the topology optimization and has previously been extensively used in the homogenization methods and the traditional boundary

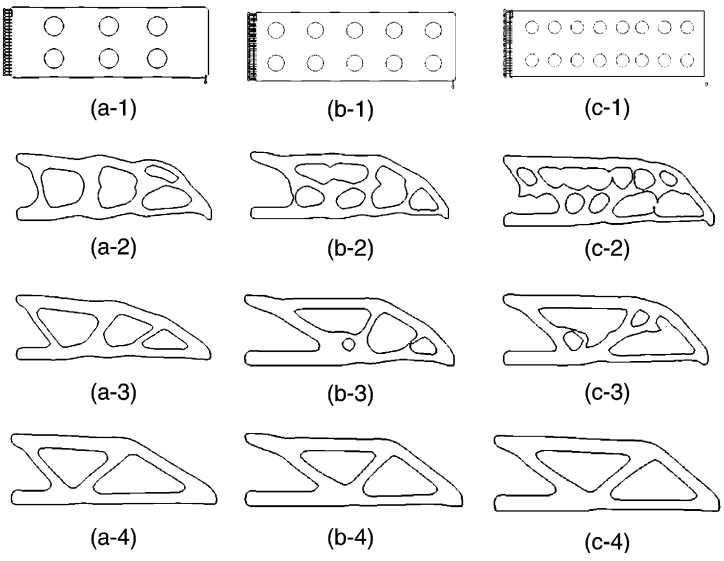

Fig. 12. The MBB beam example with three different initial conditions.

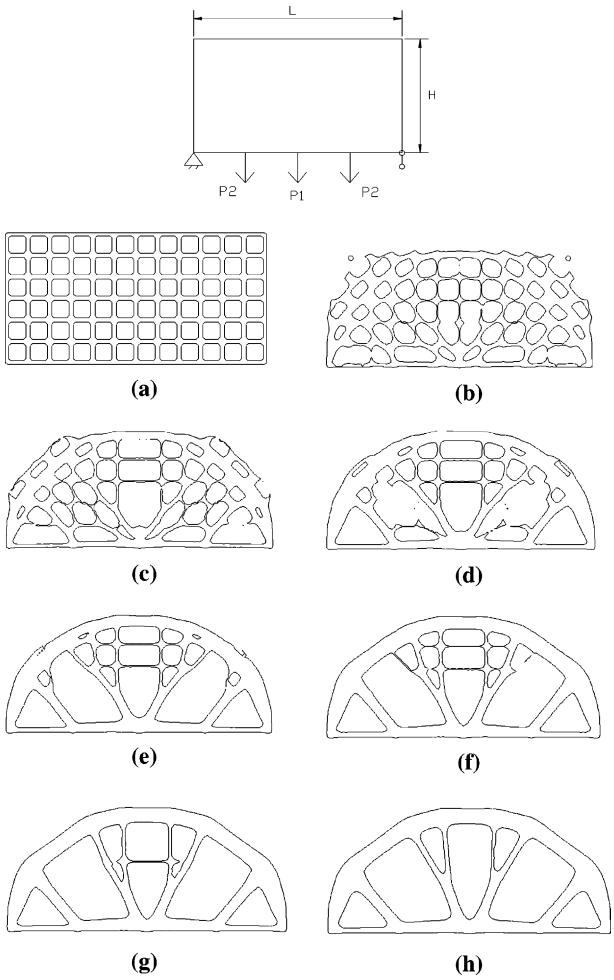

Fig. 13. A structure with multiple loads: (a) initial design, (b–g) intermediate results, and (h) final solution.

variation methods. A simply supported beam has a span of 2400 mm and a height of 400 mm, with a point load of 20 kN applied at the middle span. Due to symmetry, only half of the structure is modeled with the normal boundary conditions as shown in Fig. 12. The volume ratio is limited to 0.4. Three cases with different initial designs are studied to show that the initial conditions have a strong influence on the path of optimum solution but have little effect on the final optimal result. The iterative processes of the three cases are illustrated in Fig. 12(a:1–4), (b:1–4), and (c:1–4) respectively. A mesh of 66×22 elements is used.

8.4. Michell-type structures with multiple loads

An Michell-type structure is now considered with multiple loads at its bottom as shown in Fig. 13. The volume ratio is 0.3. A mesh of 62×122 quadrilateral elements is used for FEM analysis. In Fig. 13, the structure has a fixed and a simple support at the bottom corners with $P_1 = 30N$ and $P_2 = 5N$. The initial design and some intermediate and the final optimization results are shown.

9. Conclusions

We have presented a numerical method for structural shape and topology optimization. The method relies on a novel approach to the representation of the design boundaries with level set models. A structural optimization is formulated as a mathematical programming problem with a design objective and a set of constraints, utilizing the level set models for the incremental shape changes. The movements of the IMBs of the structure are driven by a transformation of the objective and the constraints into speed functions that govern the level set propagation. The result is a 3D topology optimization technique that demonstrates outstanding flexibility of handling topological changes, fidelity of boundary representation and degree of automation, comparing favorably with other methods based on boundary variation or homogenization in the literature.

The work presented in this paper is by no means complete. We have only implemented a direct and linear speed function. We believe that a nonlinear speed function may substantially increase computational efficiency for a faster convergence. Other numerical techniques than the narrow band method may also have a significant impact in improving the numerical accuracy and efficiency. The approach can certainly be applied to other problems of structural optimization involving multi-physics and/or multi-domains.

Acknowledgements

This research work is supported in part by the USA National Science Foundation (CMS9634717), the Chinese University of Hong Kong (Direct Research Grant 2050254), the Ministry of Education of China (a Visiting Scholar Grant at the Sate Key Laboratory of Manufacturing Systems in Xi'an Jiaotong University), and the Natural Science Foundation of China (NSFC) (grant no. 59775065 and Young Overseas Investigator Collaboration Award 50128503).

References

[1] G.I.N. Rozvany, Structural Design via Optimality Criteria, Kluwer, Dordrecht, 1988.
[2] M.P. Bendsoe, N. Kikuchi, Generating optimal topologies in structural design using a homogenisation method, Computer Methods in Applied Mechanics and Engineering 71 (1998) 197–224.
[3] K. Suzuki, N. Kikuchi, A homogenization method for shape and topology optimization, Computer Methods in Applied Mechanics and Engineering 93 (1991) 291–381.
[4] A.R. Diaz, M.P. Bendoe, Shape optimization of structures for multiple loading conditions using a homogenization method, Structural Optimization 4 (1992) 17–22.
[5] G. Allaire, R.V. Kohn, Topology optimization and optimal shape design using homogenization, in: M.P. Bendsoe, C.A. Moa Soares (Eds.), Topology Design of Structures, NATO ASI Series, Series E, vol. 227, Kluwer, Dordrecht, 1993, pp. 207–218.
[6] M.P. Bendsoe, R. Haber, The Michell layout problem as a low volume fraction limit of the homogenization method for topology design: An asymoptotic study, Structural Optimization 6 (1993) 63–267.
[7] G. Allaire, The homogenization method for topology and shape optimization, in: G.I.N. Rozvany (Ed.), Topology Optimization in Structural Mechanics, GISM, 1997, pp. 101–133.
[8] M.P. Bendsoe, Optimization of Structural Topology, Shape and Material, Springer, Berlin, 1997.
[9] M.P. Bendsoe, Optimal shape design as a material distribution problem, Structural Optimization 1 (1989) 193–202.
[10] H.P. Mlejnek, Some aspects of the genesis of structures, Structural Optimization 5 (1992) 64–69.
[11] M.P. Bendsoe, O. Sigmund, Material interpolations in topology optimization, Archive of Applied Mechanics 69 (1999) 635–654.
[12] Y.M. Xie, G.P. Steven, A simple evolutionary procedure for structural optimization, Computers and Structures 49 (1993) 885–896.
[13] D.N. Chu, Y.M. Xie, A. Hira, G.P. Steven, On various aspects of evolutionary structural optimization for problems with stiffness constraints, Finite Elements in Analysis and Design 24 (1997) 197–212.
[14] D. Reynolds, J. McConnachie, P. Bettess, W.C. Christie, J.W. Bull, Reverse adaptivity—A new evolutionary tool for structural optimization, International Journal of Numerical Methods in Engineering 45 (1999) 529–552.

[15] H.A. Eschenauer, H.A. Kobelev, A. Schumacher, Bubble method for topology and shape optimization of structures, Structural Optimization 8 (1994) 142–151.
[16] H.A. Eschenauer, A. Schumacher, Topology and shape optimization procedures using hole positioning criteria, in: G.I.N. Rozvany (Ed.), Topology Optimization in Structural Mechanics, GISM, 1997, pp. 135–196.
[17] J.A. Sethian, A. Wiegmann, Structural boundary design via level set and immersed interface methods, Journal of Computational Physics 163 (2) (2000) 489–528.
[18] J.A. Sethian, Level Set Methods and Fast Marching Methods: Evolving Interfaces in Computational Geometry, Fluid Mechanics, Computer Vision, and Materials Science, Cambridge University Press, 1999.
[19] S. Osher, J.A. Sethian, Front propagating with curvature-dependent speed: Algorithms based on Hamilton–Jacobi formulations, Journal of Computational Physics 79 (1988) 12–49.
[20] S. Osher, R. Fedkiw, Level set methods: An overview and some recent results, Journal of Computational Physics 169 (2001) 475–502.
[21] D. Breen, R. Whitaker, A level set approach for the metamorphosis of solid models, IEEE Transactions on Visualization and Computer Graphics 7 (2) (2001) 173–192.
[22] G. Rozvany, Aims, scope, methods, history and unified terminology of computer aided topology optimization in structural mechanics, Structural and Multidisciplinary Optimization 21 (2001) 90–108.